Antenna Modeling Using 3D Hybrid Finite Element - Finite Difference Time Domain Method

Neelakantam Venkatarayalu [1,3], Yeow-Beng Gan [1], Robert Lee [2], Le-Wei Li [3]
[1] *Temasek Laboratories, National Univeristy of Singapore*
5, Sports Drive 2,Singapore 117508, tslnv@nus.edu.sg.
[2] *Department of Electrical and Computer Engineering, The Ohio State University*
Columbus, OH 43210, USA.
[3] *Department of Electrical and Computer Engineering , National University of Singapore*
4 Engineering Drive 3, Singapore 117576.

Abstract

3D Hybrid Finite Element - Finite Difference Time Domain (FE/FDTD) Method is developed and applied to the numerical modeling of antennas. The antenna geometry is modeled using tetrahedral finite element mesh. Pyramidal elements are introduced in the transition from unstructured tetrahedral elements to structured hexahedral elements. The finite element formulation incorporates the excitation of antennas using coaxial line or stripline ports with Transverse Electromagnetic Mode (TEM). Computation of reflection coefficient of typical antennas is presented.

1. INTRODUCTION

With requirements on antenna characteristics becoming more complex due to pervasive use of wireless communication devices, numerical modeling of antennas becomes an integral and vital step in antenna design. Efficient numerical techniques for more accurate modeling of complex antennas and their radiation phenomena are in need, more than before. The finite difference time domain (FDTD) algorithm is a popular numerical method. The algorithm gained popularity mainly due to the following reasons viz., a) it is explicit in nature, i.e., the solution does not require any matrix inversion; b) Mesh generation is relatively easy as compared to unstructured mesh generation; c) ability to handle material inhomogeneity is inherent; d) Courant condition for numerical stability is well established; e) Easier implementation of Perfectly Matched Layer(PML) to model unbounded problems. However, the major limitation of the method lies with the staircasing errors due to the structured cartesian nature of the computational grid. The modeled geometry must conform to the grid, in contrast to numerical methods based on unstructured grids, such as finite element method (FEM). FEM is well-established and widely used for time-harmonic solution of Maxwell's equations. In comparison, the Finite Element Time Domain (FETD) method [1],[8] gains popularity only recently. The unstructured nature of the time domain version of FEM gives a clear advantage over FDTD in modeling complex antenna geometeries. Although most of the concepts developed for FEM in the frequency domain can be extended to its time domain counterpart, the numerical implementation of FETD is complicated and often inefficient. For instance, the implementation of the widely used PML in frequency domain FEM and FDTD methods is not straightforward in FETD. Apart from the difficulty in the implementation of PML in FETD, another disadvantage is the implicit nature of the field update equations. FETD method requires a matrix solution at each time step. The hybrid FE/FDTD method [3],[4] overcomes the disadvantage of FETD viz., modeling of PML for unbounded problems and that of FDTD viz., inaccuracy in modeling of complicated geometeries. In this paper, we show some results obtained in modeling certain antennas using the hybrid FE/FDTD method. The hybrid algorithm involves introduction of pyramidal elements to provide a conforming interface between the FDTD cartesian grid and finite element tetrahedral mesh. The requirement on mesh generation for the hybrid algorithm and a simple strategy that we use are briefly discussed. Modeling of antenna feed structure which support transverse electromagnetic mode (TEM) and extraction of input impedance will be presented. Finally, the method is applied to compute the input impedance of some typical antennas.

2. HYBRID FE/FDTD METHOD

FETD method uses tangential vector edge element basis functions for the electric field on a tetrahedral mesh. On the other hand, FDTD has both electric and magnetic field unknowns on two regular but staggered cartesian grids. Each FDTD cell can be treated as a hexahedral element with the electric field unknowns placed on the edges. When interfacing the FDTD and FETD grids with tetrahedral elements, conformity of certain tetrahedral edges is lost. These edges are basically along the diagonal of the rectangular face of FDTD cell, as shown in Fig. 1(a). In [2], a second order accurate interpolation is used for the diagonal edge (non-conforming) unknowns based on the four FDTD unknowns along the edges of rectangular face. These unknowns were used as Dirichlet boundary condition for the FETD update. The algorithm was reported to be numerically unstable. A stable hybridization of FETD

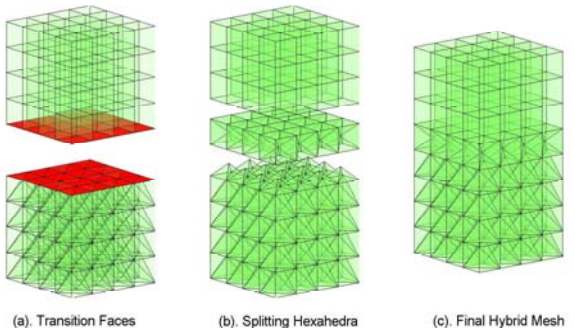

Fig. 1: Steps involved in Hybrid Mesh Generation.

and FDTD based on the equivalence between FDTD and FETD on hexahedral elements under the following conditions viz., a) using trapezoidal rule to evaluate the integrals for mass and stiffness matrices of hexahedral elements, and b) using $\theta = 0$ in the $\theta-$scheme [1] for temporal discretization was implemented in [3],[4]. This method, however, would require introduction of pyramidal elements to eliminate non-conforming diagonal edges in the transition from tetrahedral to hexahedral elements.

A. Hybrid Mesh Generation

The first step in the hybrid mesh generation involves basic unstructured tetrahedral mesh generation of the antenna structure. Outer boundary of the tetrahedral mesh must have a surface triangulation consistent with the FDTD cell size, Δh. Layer of hexahedral elements with edge length Δh is then added around the tetrahedral mesh. In the interface between tetrahedral and hexahedral elements, the only non-conforming edges(tetrahedral) must form the diagonals of the hexahedral faces on the interface. The fact that this requirement is not guranteed in general by most of the available unstructured mesh generators remains a major hurdle in the application of the hybrid algorithm. Fig. 1(a), shows the hexahedral and tetrahedral regions of the mesh, separated to show the rectangular and triangular faces on their interface. The number of nodes on the interface from the tetrahedral mesh and the hexahedral mesh are the same. The number of edges on the tetrahedral interface is greater than the number of edges on the hexahedral interface by the number of rectangular faces on the interface. Once such a mesh is generated, hexahedral elements with a face on the interface is split into two tetrahedra and five pyramidal elements, as shown in Fig. 1(b), leading to the final hybrid mesh shown in Fig. 1(c).

B. Pyramidal Edge Elements

Edge vector basis functions has been used extensively on tetrahedral and hexahedral elements. For the 3D Hybrid FE/FDTD

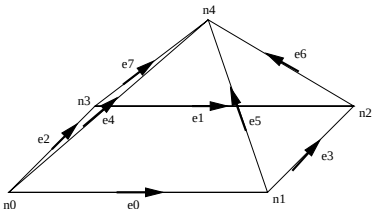

Fig. 2: Pyramidal element with reference node and edge numbering.

method, similar basis functions are defined over the pyramidal elements. Edge vector basis functions on pyramidal elements was designed in [6]. Each basis function is associated with a particular edge of the pyramidal element, similar to edge vector basis functions on tetrahedral elements. Thus, each pyramidal element has eight degrees of freedom, corresponding to the number of edges. With reference to Fig. 2, the edge basis functions are given as

$$\vec{W}_{ij} = \xi_i \nabla(\xi_j + \xi_k) - \xi_j \nabla(\xi_i + \xi_l) \tag{1}$$

for the four edges on the base of the pyramidal element formed by the nodes i, j, k, l and

$$\vec{W}_{ij} = \xi_i \nabla \xi_j - \xi_j \nabla \xi_i \tag{2}$$

for the other four oblique edges of the pyramid. ξ_i is the nodal shape function of unit value at node i and zero at other nodes [6]. In the transition from tetrahedral to hexahedral elements with edge length Δh, only a particular class of pyramidal elements of height $\Delta h/2$ and a square base of sidelength Δh are generated. Once the basis funtions for such pyramids are defined, their mass and stiffness matrices can be evaluated using a symbolic computation tool such as Mathematica®, and is obtained as

$$T^e = \frac{\Delta h}{4320} \begin{pmatrix} 192 & 96 & 12 & -12 & -9 & 9 & 9 & -9 \\ 96 & 192 & -12 & 12 & -9 & 9 & 9 & -9 \\ 12 & -12 & 192 & 96 & -9 & -9 & 9 & 9 \\ -12 & 12 & 96 & 192 & -9 & -9 & 9 & 9 \\ -9 & -9 & -9 & -9 & 308 & 160 & 92 & 160 \\ 9 & 9 & -9 & -9 & 160 & 308 & 160 & 92 \\ 9 & 9 & 9 & 9 & 92 & 160 & 308 & 160 \\ -9 & -9 & 9 & 9 & 160 & 92 & 160 & 308 \end{pmatrix} \tag{3}$$

and

$$S^e = \frac{1}{18\Delta h} \begin{pmatrix} 17 & 7 & -1 & 1 & -16 & 16 & 8 & -8 \\ 7 & 17 & 1 & -1 & -8 & 8 & 16 & -16 \\ -1 & 1 & 17 & 7 & -16 & -8 & 8 & 16 \\ 1 & -1 & 7 & 17 & -8 & -16 & 16 & 8 \\ -16 & -8 & -16 & -8 & 32 & -8 & -16 & -8 \\ 16 & 8 & -8 & -16 & -8 & 32 & -8 & -16 \\ 8 & 16 & 8 & 16 & -16 & -8 & 32 & -8 \\ -8 & -16 & 16 & 8 & -8 & -16 & -8 & 32 \end{pmatrix} \tag{4}$$

In general, there are six possible orientations for the pyramidal elements in the hybrid mesh. The mass and stiffness matrices are independent of its orientation.

C. Port Modeling

The antenna structure is located in the finite element region. Hence, the FETD formulation must include the excitation of antenna using ports. The FETD method used in this paper

can model the excitation of transverse electromagnetic mode (TEM) in coaxial line or stripline feed. Such feed are typically used for antennas operating with TEM mode, and hence, higher order modes (which are evanescent) can be neglected. However, the transmission line should be sufficiently long for the higher order modes to attenuate significantly [7]. In the time-harmonic case, the total electric fields inside a transmission line exciting a TEM wave in the $+z$ direction is given by

$$\begin{aligned}\vec{E} &= \vec{E}^{inc} + \vec{E}^{ref} \\ &= E_o \vec{e}_{TEM} e^{-j\beta z} + \Gamma E_o \vec{e}_{TEM} e^{j\beta z} \end{aligned} \quad (5)$$

where $\vec{e}_{TEM}$ is the modal field distribution, E_o is the incident modal amplitude, Γ is the reflection coefficient of TEM mode and β is the propagation constant of the TEM mode inside the transmission line. For dielectric filled coaxial lines and striplines, $\beta = \sqrt{\varepsilon_r} k_0 = \sqrt{\varepsilon_r}\omega/c$ where ε_r is the dielectric constant of the medium. From (5),

$$\hat{n} \times \nabla \times \vec{E} = j\beta\gamma_t(\vec{E}) - 2j\beta\gamma_t(\vec{E}^{inc}) \quad (6)$$

where $\hat{n} = -\hat{z}$ is the outward normal unit vector and $\gamma_t(\vec{u}) = \hat{n} \times \vec{u} \times \hat{n}$ is the tangential trace of $\vec{u}$. From (6), the time-dependent boundary condition for the electric field in a port (filled with non-magnetic material) excited by TEM mode is obtained as

$$\hat{n} \times \nabla \times \vec{E}(t) = \frac{\sqrt{\varepsilon_r}}{c}\frac{\partial}{\partial t}\gamma_t(\vec{E}(t)) - \frac{2\sqrt{\varepsilon_r}}{c}\frac{\partial}{\partial t}\gamma_t(\vec{E}^{inc}(t)) \quad (7)$$

Thus, the initial value problem in the FETD region is the time-dependent vector Helmholtz's equation

$$\nabla \times \mu_r^{-1} \nabla \times \vec{E}(t) + \frac{\varepsilon_r}{c^2}\frac{\partial^2}{\partial t^2}\vec{E}(t) = 0, \quad \text{in } \Omega \quad (8)$$

with the boundary condition (7) on the port surface and the initial conditions $\vec{E}(0) = 0$ and $\frac{\partial}{\partial t}\vec{E}(t)|_{t=0} = 0$. Testing (8) with suitable test function results in the following weak form viz.,
seek $\vec{E}(t)$ such that

$$\begin{aligned}\int_\Omega \left[\nabla \times \vec{v}(t) \cdot \mu_r^{-1} \nabla \times \vec{E}(t) + \frac{\varepsilon_r}{c^2}\vec{v}(t) \cdot \frac{d^2}{dt^2}\vec{E}(t)\right] d\Omega \\ + \int_{\Gamma_p} \vec{v}(t) \cdot (\hat{n} \times \nabla \times \vec{E}(t)) ds = 0 \end{aligned} \quad (9)$$

$\forall \vec{v}(t) \in \mathcal{H}(curl; \Omega)$.

Using (7) in (9) with $\vec{E}^{inc}(t) = E_o(t)\vec{e}_{TEM}$ and expanding the solution $\vec{E}(t)$ using edge element basis functions defined over tetrahedral, pyramidal and hexahedral elements as $\vec{E}(t) = \sum_{i=1}^{N} e_i(t)\vec{W}_i$ leads to the following system of ordinary differential equation viz.,

$$\mathbf{S}\mathbf{e} + \frac{1}{c}\mathbf{R}\frac{d}{dt}\mathbf{e} + \frac{1}{c^2}\mathbf{T}\frac{d^2}{dt^2}\mathbf{e} = \frac{2}{c}\mathbf{f}\frac{d}{dt}E_o(t) \quad (10)$$

where

$$\begin{aligned}\mathbf{S}(i,j) &= \int_\Omega \nabla \times \vec{W}_i \cdot \mu_r^{-1} \nabla \times \vec{W}_j \, d\Omega \\ \mathbf{T}(i,j) &= \int_\Omega \vec{W}_i \cdot \varepsilon_r \vec{W}_j \, d\Omega \\ \mathbf{R}(i,j) &= \int_{\Gamma_p} (\hat{n} \times \vec{W}_i) \cdot \sqrt{\varepsilon_r}(\hat{n} \times \vec{W}_j) \, ds \\ \mathbf{f}(i) &= \int_{\Gamma_p} (\hat{n} \times \vec{W}_i) \cdot \sqrt{\varepsilon_r}(\hat{n} \times \vec{e}_{TEM}) \, ds \end{aligned}$$

$E_o(t)$ is the excitation waveform with significant spectral contents in the frequency band of interest. The modal distribution $\vec{e}_{TEM}$ is obtained by a 2D finite element eigenvalue solver. The eigenvector solution for the dominant mode gives the modal distribution of TEM mode. For the 2D problem, the triangulation of the port surface in the tetrahedral mesh is employed as the finite element mesh. The modal distribution, expanded using 2D edge elements, is obtained as $\vec{e}_{TEM} = \sum_{j=1}^{N_p} e_{TEM,j}\vec{W}_j$ where N_p is number of unknowns for the 2D eigenvalue problem and is equal to the number of edges on the port triangulation. $\mathbf{e}_{TEM}$ is the eigenvector of the dominant mode. For the 2D modal distribution, we use the center frequency in the band of interest with the assumption that the modal distribution of the TEM mode remains unchanged within the band. This assumption is true for coaxial lines and stripline feed structures [8]. The temporal discretization of (10) is performed using the $\theta-$ method as discussed in [1].
Using the orthogonality property of the modes, we obtain the reflection coefficient from (5) as

$$\Gamma(\omega) = \frac{1}{\mathcal{F}(E_o(t))}\mathcal{F}\left(\int_{\Gamma_p} \vec{E}(t) \cdot \vec{e}_{TEM} \, ds\right) - 1 \quad (11)$$

where $\mathcal{F}(u(t))$ is the Fourier transform of $u(t)$.

3. NUMERICAL EXAMPLES

The 3D hybrid FE/FDTD code was implemented in C++ using object-oriented programming features. The FETD update matrices are stored in compressed column storage format for sparse matrices. For efficient implicit update of the FETD unknowns, complete Cholesky factorization of the matrix is performed once before the time marching begins. To reduce the number of non-zero entries in the Cholesky Factor, matrix reordering is applied [9]. Anisotropic PML is used in the FDTD region. In all examples, the maximum edge length in the finite element region is $1.5\Delta h$.

A. λ/4 Monopole

The first example is a 15mm λ/4 monopole located above a finite ground plane. The inner conductor of the coaxial line extends out as the monopole arm. The radii of inner and outer conductors of the coaxial line are 1.3mm and 3mm respectively. The geometry is shown in Fig. 3(a) and the PEC faces of finite element mesh used is shown in Fig. 3(b). Δh is set as 2mm. The input impedance of this antenna using the hybrid code is compared to the results obtained using HFSS®

(a) Geometry (b) PEC Faces

Fig. 3: Modeling of $\lambda/4$ monopole on a finite ground plane.

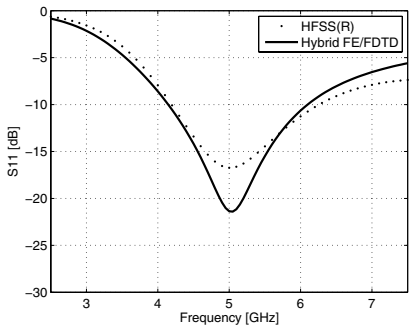

Fig. 4: Reflection Coefficient of Monopole antenna indicating the resonant frequency.

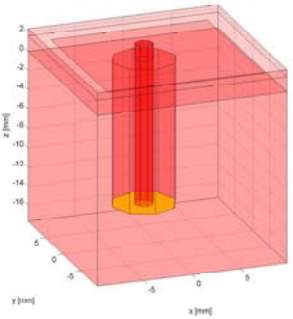

Fig. 5: Modeling of Coaxial line fed Square patch antenna.

with infinite ground plane, as shown in Fig. 4. The results are in good agreement, with both predicting resonance at about 5GHz.

B. Coax-fed Square Patch Antenna

The second example is a patch antenna. This is the unit radiating element in a JINA 2004 Test Case [10]. The 16.2mm x 16.2mm square patch is embedded in a 19.6mm x 19.6mm substrate with $\varepsilon_r = 2.2$ and thickness 2.34mm, as shown in Fig. 5. The element is inserted in a perfectly conducting cavity. Δh is set as 1mm. Reflection coefficient obtained using the hybrid code is shown in Fig. 6, where excellent agreement is achieved with results from a frequency domain FEM code.

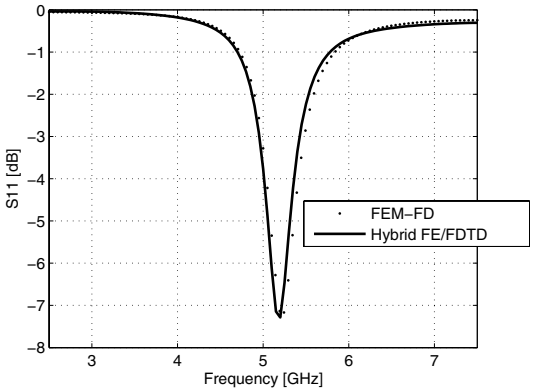

Fig. 6: Reflection Coefficient of Patch Antenna indicating the resonant frequency

4. CONCLUSION

The 3D Hybrid FE/FDTD method retains the inherent advantage of FETD in modeling arbitrarily shaped structures along with the efficiency of FDTD in modeling simple shapes and PML. Antenna feed with TEM excitation is incorporated in the FETD formulation to obtain the reflection coefficient and hence, input impedance. Initial results obtained using the method are promising and demonstrate its potential application to the design and analysis of broadband and ultrawideband antennas.

REFERENCES

[1] J.-F. Lee, R. Lee, and A. Cangellaris, "Time-domain finite-element methods," *IEEE Trans. Antennas Propagat.*, vol. 45, no. 3, 1997, pp. 430-442..

[2] R.-B. Wu and T. Itoh, "Hybrid finite-difference time-domain modeling of curved surfaces using tetrahedral edge elements," *IEEE Transactions on Antennas and Propagation*, vol. 45, no. 8, 1997, pp. 1302–1309.

[3] T. Rylander and A. Bondeson, "Stability of explicit-implicit hybrid time-stepping schemes for Maxwell's equations," *Journal of Computational Physics*, vol. 179, no. 2, 2002, pp. 426-438.

[4] S. Wang, R. Lee, F.L. Teixeira and J.F. Lee "A Hybrid Finite Element Time Domain/Finite Difference Time Domain Approach for Electromagnetic Modeling", Progress in Electromagnetics Research Symposium, Singapore, January 2003.

[5] N.-V. Venkatarayalu, Y.-B. Gan, and L.-W. Li, "Investigation of numerical stability of 2D FE/FDTD hybrid algorithm for different hybridization schemes." *IEICE Transactions on Communications*, vol. E88-B, no. 6, 2005, pp. 2341-2345.

[6] J.-L. Coulomb, F.-X Zgainski, Y. Marechal, "A Pyramidal Element to link Hexahedral, Prismatic and Tetrahedral Edge Finite Elements", *IEEE Trans. on Magnetics*, Vol. 33, No. 2, 1997, pp. 1362-1365.

[7] J. Jin, *The Finite Element Method in Electromagnetics*, 2nd ed. New York: Wiley-Interscience, 2002.

[8] D.-K. Sun, J.-F. Lee, and Z. Cendes, "The Transfinite-Element Time-Domain Method.", *IEEE Transactions on Microwave Theory and Techniques*, vol. 51, no. 10, 2003, pp. 2097–2105.

[9] G. Karypis, and V. Kumar, "METIS 4.0: Unstructured graph partitioning and sparse matrix ordering system.", *Technical Report, Department of Computer Science,* University of Minnesota, 1998. Available on the WWW at URL *http://www.cs.umn.edu/?metis.*

[10] A. Barka, and G. Salin, JINA 2004 TEST Case 8: 20x20 patch Array Antenna, Available on the WWW at URL *http://www.elec.unice.fr/pages/congres/jina2004/workshop/test8.pdf.*